Composites Research

Vol. 38, No. 4, 414-420 (2025)
DOI: http://dx.doi.org/10.7234/composres.2025.38.4.414
ISSN 2288-2103(Print), ISSN 2288-2111(Online)

Paper

Dielectric Surface Modification of NCM Cathodes Using $BaTiO_3$ for High-rate Lithium-ion Batteries

Jihye Seo*,, Soomin Kim**, Moonhee Choi*†, Yoonmook Kang**†**

ABSTRACT: Ni-rich NCM811 cathodes offer a high specific capacity but experience severe degradation under high-rate cycling owing to interfacial side reactions and structural instability. In this study, $BaTiO_3$ (BT), a high-dielectric ferroelectric, was applied as a nanodot surface coating using a room-temperature, solvent-free Resonant Acoustic Mixing (RAM) process. The RAM process enables uniform nanoparticle dispersion without requiring thermal treatment or complex post-processing, thereby providing a simple and efficient strategy for interfacial modification using dielectric coatings. NCM811 powders were coated with varying amounts of BT (1-10 wt%) and evaluated via rate capability, impedance spectroscopy, and long-term cycling. Among them, the 2 wt% composition showed the most pronounced improvement. The BT-coated electrodes exhibited consistently enhanced rate performance compared to bare NCM across all charge-discharge rates (C-rates; 0.1-10C). Notably, at 10 C, the 2 wt% BT-coated sample delivered a 14.2% higher discharge capacity, confirming superior high-rate capability. Charge transfer resistance was reduced by 51.8%, and lithium-ion diffusion improved by 107%, indicating faster reaction kinetics. Furthermore, under long-term cycling at 10 C, the coated electrode retained more than 50% of its initial capacity after 200 cycles, demonstrating improved structural and interfacial stability. These findings demonstrate that the BT nanodot coating, applied via a solvent-free and room-temperature RAM process, functions as a multifunctional interfacial layer that suppresses interfacial degradation through physical protection and enhances lithium-ion mobility by modulating local electric fields. The RAM technique enabled uniform nanodot dispersion without damaging the NCM crystal structure and offers an efficient, scalable, and post-treatment-free route for advanced lithium-ion battery cathode design.

Key Words: Lithium-ion battery, Ni-rich cathode, $BaTiO_3$ coating, Resonant acoustic mixing, High-rate cycling

1. INTRODUCTION

Lithium-ion batteries (LIBs), known for their high energy density and long cycle life, are widely utilized as essential energy storage systems in various applications, including portable electronics, electric vehicles (EVs), and energy storage systems (ESSs) [1,2]. In particular, for applications requiring high-rate charge/discharge, such as EVs and ESSs, the lithium-ion diffusion rate and interfacial resistance of the electrode materials play critical roles in determining battery performance [3].

Among various cathode materials essential for improving LIB performance, Ni-rich layered oxide $LiNi_{0.8}Co_{0.1}Mn_{0.1}O_2$ (NCM811) has garnered attention due to its high theoretical capacity (~275 mAh g^{-1}) and energy density. However, Ni-rich NCM cathodes (Ni ≥ 80%) experience low initial coulombic efficiency and capacity fading due to surface residual lithium compounds and cation mixing [4,5]. In particular, under high-rate charge/discharge and high-voltage (e.g., 4.5 V) operating conditions, complex challenges, such as interfacial reactions with electrolytes, increased charge transfer resistance, and structural degradation of particles, can result in rapid performance deterioration [6].

To address these challenges, surface coating strategies using inorganic materials have been proposed to enhance chemical stability at the cathode-electrolyte interface [7]. Materials, such as TiO_2, Al_2O_3, ZrO_2, and Li_3PO_4, have demonstrated effectiveness in improving cycle life by suppressing interfacial reac-

Received 26 June 2025, received in revised form 15 July 2025, accepted 23 July 2025

*Electronic Convergence Division, Korea Institute of Ceramic Engineering & Technology, Jinju 52851, Korea
**Graduate School of Energy and Environment, Korea University, Seoul 02841, Korea
†Corresponding author (E-mail: moonhee77, choi@kicet.re.kr (Moonhee Choi); E-mail: ddang@korea.ac.kr (Yoonmook Kang))

tions [8, 9]. However, most of these coatings exhibit low lithium-ion conductivities or insulating properties, which limit their effectiveness under high-rate conditions [10,11].

As an alternative, $BaTiO_3$ (BT), a ferroelectric material with a high dielectric constant, has recently attracted attention [12, 13]. BT induces a localized electric field at the interface, thereby facilitating lithium-ion migration and suppressing side reactions with the electrolyte. Although BT is inherently insulating, when applied in the form of dispersed nanodots, it can contribute to interfacial stabilization without hindering Li^+ transport [14]. Previous studies have reported that BT coatings can effectively suppress a Cathode Electrolyte Interphase (CEI), induce lithium vacancies, and enhance lithium-ion diffusion coefficients [15,16].

However, conventional coating processes rely on high-temperature annealing or solvent-based wet processes, which introduce limitations, such as high processing costs, long treatment times, environmental concerns, and procedural complexity [17]. In particular, organic solvents pose risks because of their flammability, toxicity, and significant disposal costs, whereas aqueous-based systems are hindered by high energy consumption owing to the large latent heat of vaporization of water and limited applicability to moisture-sensitive materials [18,19]. To overcome these drawbacks, this study introduces Resonant Acoustic Mixing (RAM), a room-temperature, solvent-free technique that can achieve uniform nanoparticle dispersion and surface coating within seconds using low-frequency acoustic energy. RAM offers several advantages, including the elimination of heat treatment, minimized particle damage, and reduced processing time [20].

In this study, nanostructured BT was coated onto polycrystalline NCM811 particles using RAM with varying contents (1–10 wt%), and the resulting electrochemical performance was systematically investigated. This approach evaluates the potential of a dielectric coating strategy to improve the cycle performance and lithium-ion diffusion characteristics of Ni-rich cathode materials and demonstrates its applicability as a simple, low-cost, and efficient coating technique that does not require complex processing.

2. EXPERIMENTALS

2.1 Solvent-free Surface Coating of NCM811 Using Resonant Acoustic Mixing (RAM)

Commercial NCM811 powder (d_{50} = 11.4 μm, POSCO Future M, Korea) was mixed with BT powder (d_{50} = 250 nm, KCM Co., Japan) at designated weight ratios without any pretreatment. The mixed powders were filled into a container to over 60% of their volume and processed using a Resonant Acoustic Mixer (LabRAM, Resodyn Acoustic Mixers, USA) under 60 G acceleration for 20 min. This process induced particle–particle collisions and friction through strong vibrations, which promoted the uniform dispersion and adhesion of BT onto the surface of the NCM811 particles. The final coated powders were used without any additional heat treatment. A schematic of the RAM coating process is shown in Fig. 1.

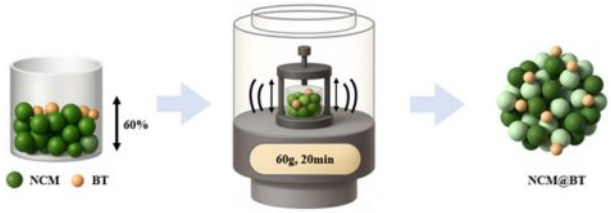

Fig. 1. Fabrication process of NCM and BT coating via the RAM method

2.2 Electrochemical Evaluation of BT-Coated NCM811 Composite Cathodes

Composite cathode slurries were prepared using both the BT-coated and bare NCM811 powders. The active material (NCM811), conductive carbon (Super P, IMERYS Graphite & Carbon, France), and binder (PVDF, Typolymer Co., Korea) were mixed at a weight ratio of 8:1:1 using N-methyl-2-pyrrolidone (NMP, 99%, Sigma-Aldrich, USA) as the solvent. The resulting slurries were uniformly cast onto aluminum foil using a doctor blade, dried at 80°C in a vacuum oven, and subsequently roll-pressed to obtain the desired thickness. Circular electrodes (14 mm diameter) were punched from the dried films.

Cell assembly was conducted in an argon-filled glove box (LABstar, MBraun), where H_2O and O_2 concentrations were kept below 0.1 ppm. Coin-type 2023 half-cells were developed using lithium metal (0.3 mm thick, >99.9%, MTI Korea) as the counter electrode and 1 M $LiPF_6$ dissolved in EC/DMC/DEC (1:1:1, v/v/v; Enchem Co., Korea) as the electrolyte. After assembly, the cells were aged at 60°C for 12 h before electrochemical testing. All the electrochemical tests were conducted at room temperature within a voltage range of 3.0-4.5 V.

3. RESULTS AND DISCUSSION

3.1 Optimization of $BaTiO_3$ Coating on NCM Cathodes

Fig. 2 presents the surface analyses of the BT-coated NCM811 composite cathode materials using field-emission scanning electron microscopy (FE-SEM) and energy-dispersive X-ray spectroscopy (EDS) after coating via the RAM process. The FE-SEM images show that the NCM particles retained their typical polyhedral morphology, with no noticeable particle fracture or structural collapse after vibrational coating (60 G, 20 min). This indicates that the RAM process did not induce any mechanical degradation, such as microcracks or particle detachment, confirming its suitability as a gentle and nondestructive surface modification method. EDS elemental

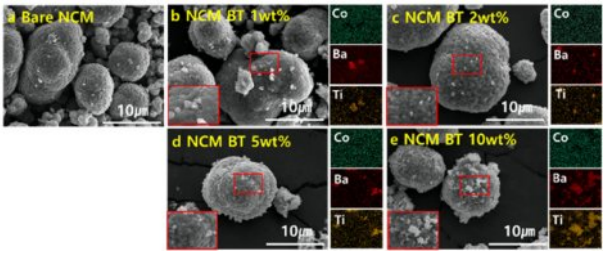

Fig. 2. Field-emission SEM and corresponding EDS elemental mapping results of BT-coated NCM811 powders prepared via RAM process with varying BT contents: (a) 0 wt%, (b) 1 wt%, (c) 2 wt%, (d) 5 wt%, (e) 10 wt%

Table 1. I(003)/I(104) intensity ratios of BT-coated and bare NCM811 samples for evaluating layered structure integrity

NCM	Bare	BT 1 wt%	BT 2 wt%	BT 5 wt%	BT 10 wt%
I(003)/I(104)	2.0	2.1	2.3	1.9	2.1

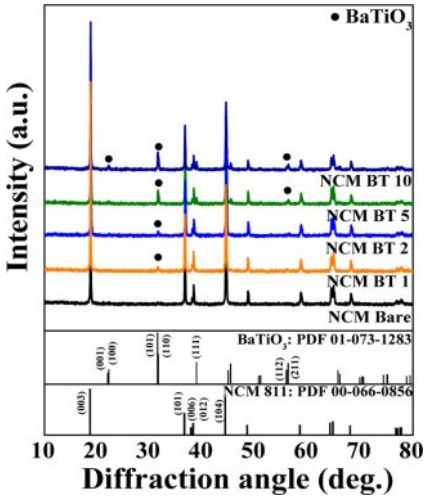

Fig. 3. XRD patterns of bare and BT-coated NCM811 powders prepared via RAM process with varying BT contents (1, 2, 5, and 10 wt%)

mapping confirmed the presence of Ba and Ti on the particle surfaces, indicating that the BT was effectively coated. Furthermore, as the BT content increased from (a) to (e), a progressive increase in the surface coverage of BT particles was observed. Specifically, uncoated surfaces were observed at 0 wt% (a), partial surface coverage appeared at 1 wt% (b), uniform and continuous coatings were formed at 2–5 wt% (c–d), and excessive BT particle aggregation was evident at 10 wt% (e).

Fig. 3 shows the X-ray diffraction (XRD, X'Pert PRO MPD, Bruker, USA) analysis results of the NCM811 composite powders used to investigate the effect of the presence and content of the BT coating on their crystal structures. All samples exhibited distinct diffraction peaks corresponding to the typical α-$NaFeO_2$-type layered structure of NCM, indicating that the BT coating process did not affect the crystal structure.

In the BT-coated samples, the characteristic diffraction peaks of BT were partially observed, and their relative intensities increased with increasing BT content. This confirmed the increasing amount of BT present on the NCM surface, as evidenced by the XRD data.

The layered structure of NCM was further confirmed by the clear peak splitting of the (006)/(102) and (108)/(110) doublets and I (003)/I (104) intensity ratio, as summarized in Table 1. Generally, an I(003)/I(104) ratio greater than 1.2 indicates a well-maintained layered structure with suppressed Li/Ni cation mixing [21,22].

In this study, all the samples exhibited ratios above 1.9, indicating that a stable layered structure was preserved regardless of the BT coating content [23]. Notably, the 2 wt% BT-coated sample showed the highest ratio of 2.3, suggesting that an optimal amount of BT coating can enhance surface stabilization and lattice ordering. In contrast, the 5 wt% BT-coated sample showed a slightly lower ratio than that of bare NCM811; however, the difference was small and likely within the experimental error. These results indicate that the crystal structure remained stable even with an increased BT coating content, and all the samples maintained high structural integrity.

Additionally, as the BT content increased, the intensity of the (006) peak of NCM811 gradually increased. In samples with 5 wt% BT or higher, the (006) peak became more intense than the (012) peak. This increase may be attributed to a combination of preferred orientation along the c-axis and the superposition of the (111) peak of $BaTiO_3$, which shares a similar 2θ value (~38.9°) [24]. Therefore, the enhancement of the (006) peak intensity can be interpreted as a result of both structural rearrangement and peak overlap.

To compare the electrochemical performance of NCM samples under various C-rate conditions (0.1–10 C; 1C = full charge/discharge in 1 hour), charge–discharge tests were conducted in the voltage range of 3.0–4.5 V using a constant current/constant voltage (CC/CV) charging mode. Fig. 4a presents the rate capabilities of the bare NCM and BT-coated samples with BT contents ranging from 1 to 10 wt%. All the samples exhibited a typical trend of decreasing discharge capacity with increasing current rate. Nevertheless, the BT-coated samples demonstrated superior overall performance compared to bare NCM. In particular, the NCM BT 2 sample, with 2 wt% BT coating, delivered discharge capacities of 196.3 mAh g^{-1} at 1C and 144.2 mAh g^{-1} at 10C, representing approximately 5.7% and 14.2% improvements over bare NCM (1C: 185.8 mAh g^{-1}, 10C: 126.3 mAh g^{-1}), respectively. These results indicate that the BT coating effectively enhances lithium-ion diffusion and reduces the interfacial resistance, thereby improving the electrochemical performance even under high-rate charge–discharge conditions.

Additionally, the capacity recovery rate was evaluated based on the discharge capacity measured after reverting to 0.1C following high-rate cycling at 10C. The recovery ratio reflects

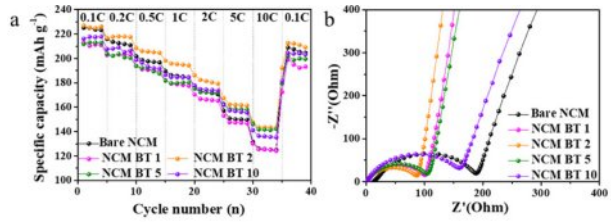

Fig. 4. (a) Rate performance of bare NCM and BT-coated NCM811 cathodes with varying BT contents (1, 2, 5, and 10 wt%), (b) Nyquist plots obtained from electrochemical impedance spectroscopy (EIS) of the same electrode

the degree of reversible capacity retention under low-rate conditions after high-rate stress. The NCM BT 2 sample exhibited the highest recovery of approximately 92%, which was approximately 3% higher than that of bare NCM (89%). These results suggest the superior resilience of NCM BT 2 against the structural degradation and irreversible lithium loss commonly induced under extreme rate conditions.

In contrast, both insufficient and excessive amounts of BT coating resulted in discharge capacities that were either comparable to or lower than those of the bare NCM. At a low coating level of 1 wt%, the performance degradation can be attributed to non-uniform and discontinuous coating coverage, which may disrupt the electronic conduction pathways or locally hinder Li^+ transport across the electrode–electrolyte interface. Conversely, excessive coatings, such as 5 wt% and 10 wt%, can form thick insulating BT layers that impede the transport of both ions and electrons, resulting in increased interfacial resistance and reduced electrochemically active surface area [25].

This result is further corroborated by the Electrochemical Impedance Spectroscopy (EIS) analysis, as shown in Fig. 4b. The NCM sample coated with 2 wt% BT exhibited a significantly smaller semicircle diameter compared to the bare NCM, with a charge transfer resistance (R_{ct}) of 84.5 Ω, representing a 51.8% reduction relative to that of the bare NCM (175.4 Ω). While the 1 wt% sample also demonstrates a lower R_{ct} (98.0 Ω) than the bare NCM, its resistance remains higher than that of the 2 wt% sample. As the BT content increased, the semicircle diameter gradually expanded again, and the 5 wt% and 10 wt% samples exhibited R_{ct} values of 102.0 Ω and 158.2 Ω, respectively. These results indicate that an optimal coating amount is essential to balance the interfacial resistance and charge-transfer efficiency, with 2 wt% BT confirmed as the most effective condition in this study.

In summary, the improved electrochemical performance observed at 2 wt% BT is not solely due to the optimized coating thickness but is more fundamentally attributed to a composition that enables the ferroelectric properties of BT to be most effectively expressed. Specifically, the high dielectric constant under these conditions modulates the electric field distribution at the electrode–electrolyte interface and mitigates local lithium-ion concentration gradients, resulting in more efficient ion conduction pathways [15,26]. These benefits were experimentally validated through increased discharge capacity at 10C and a significant reduction in R_{ct}. Thus, the 2 wt% BT composition was considered the most effective for achieving both interfacial stability and enhanced electrochemical reactivity. Accordingly, further electrochemical analyses were conducted by comparing bare NCM with 2 wt% BT-coated NCM (denoted as NCM@BT).

3.2 Electrochemical Evaluation of Bare and Coated NCM Cathodes

Fig. 5a presents the discharge voltage profiles at 1C and 10C for bare NCM and NCM@BT, corresponding to the samples shown in Fig. 4a. Compared to bare NCM, the NCM@BT sample exhibits consistently higher discharge voltages and a more gradual voltage drop at both current rates. Notably, under the high-rate 10C condition, bare NCM shows a sharp voltage drop and significant capacity loss, whereas NCM@BT maintains a more stable voltage profile and delivers approximately 14.2% higher discharge capacity. This improvement is attributed to enhanced charge transfer and electrochemical reaction efficiency, resulting from reduced interfacial resistance and stabilized Li^+ diffusion pathways provided by the BT coating.

To further investigate the electrochemical behavior, cyclic voltammetry (CV) analysis was performed at a scan rate of 0.1 mV s^{-1}, and the results are shown in Fig. 5b. All samples exhibit characteristic redox peak pairs typical of the NCM811 system within the voltage range of 3.0–4.5 V, indicating reversible lithium intercalation/deintercalation behavior. The oxidation (V_a) and reduction (V_c) peak potentials of bare

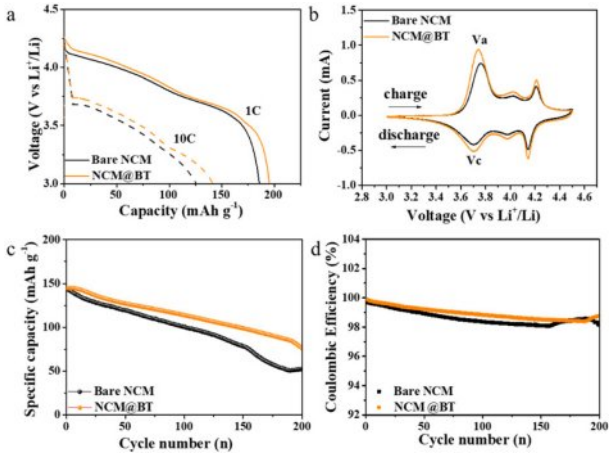

Fig. 5. Electrochemical performance comparison between bare NCM and NCM@BT (2 wt% BT-coated NCM) (3.0–4.5 V): (a) Discharge profiles at 1 C and 10 C, (b) Cyclic voltammetry (CV) curves at 0.1 mV s^{-1}, (c) Long-term cycling performance at 10 C over 200 cycles, (d) Coulombic efficiency corresponding to (c)

NCM and NCM@BT were observed at 3.761 and 3.705 V, and 3.741 and 3.706 V, respectively, resulting in corresponding potential differences (ΔV) of 0.056 V and 0.035 V. This potential gap generally reflects the degree of electrochemical polarization within the electrode, suggesting that BT coating reduces polarization in NCM and improves the reversibility of the redox reactions [22,27]. Furthermore, the NCM@BT sample exhibits higher peak current density and a larger enclosed area compared to the bare NCM, indicating faster charge transfer and improved Li^+ insertion/extraction behavior, thereby contributing to enhanced energy storage capability and electrochemical activity [28].

Fig. 5c and 5d illustrate the long-term cycling stability and coulombic efficiency (CE) evolution of the bare NCM and NCM@BT electrodes at 10 C conditions over 200 cycles. All cells were charged within a voltage window of 3.0–4.5 V in CC/CV mode, and five pre-cycling steps at 0.1C were conducted to ensure electrochemical activation and interfacial stabilization before long-term cycling. The initial discharge capacities of bare NCM and NCM@BT were 143.1 mAh g^{-1} and 144.5 mAh g^{-1}, respectively, indicating comparable initial performance. As the cycles progressed, both electrodes exhibited a gradual capacity decrease, reaching 52.4 mAh g^{-1} (bare NCM) and 75.9 mAh g^{-1} (NCM@BT) after 200 cycles. The corresponding capacity retentions were 36.3% for bare NCM and 52.6% for NCM@BT, corresponding to an improvement of approximately 44.9%. This result indicates that the BT coating significantly enhances the long-term cycling stability.

This result correlated with the CE trends is shown in Fig. 5d. As cycling proceeded, both samples exhibited a gradual decrease in the CE. However, a slight and non-linear increase in the CE was observed around the 162nd cycle for bare NCM and 188th cycle for NCM@BT, after which the CE declined again. This variation in the CE is more likely attributed to normal fluctuations within the measurement range caused by experimental noise or minor interfacial reactions rather than a true sign of CE recovery. However, considering the concurrent rapid capacity decline, this can be interpreted as a sign of pronounced degradation.

In particular, the high cutoff voltage (4.5 V) employed in this study is regarded as a major contributor to the accelerated degradation of the electrode. In Ni-rich NCM systems, such as NCM811, operating at high voltages can induce oxygen release and surface oxidation, promoting CEI instability and phase transitions [29]. These high-voltage conditions also hinder Li^+ diffusion, increase CEI thickness, and accelerate electrolyte decomposition, thereby exacerbating capacity fading and CE deterioration [30,31].

In addition, the poor long-term stability of the bare NCM electrode was attributed to mechanical stress and microcrack formation caused by repeated lattice contraction and expansion during cycling. These structural changes resulted in the formation of an inhomogeneous and thick CEI, which consumes active Li and causes irreversible capacity loss and reduced CE [32].

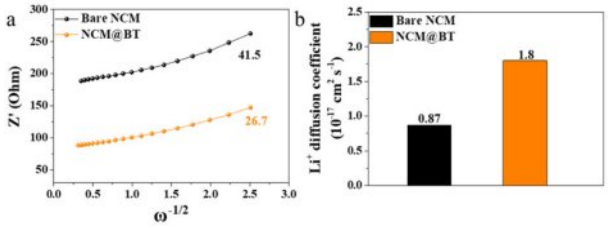

Fig. 6. Lithium-ion diffusion characteristics of bare NCM and NCM@BT: (a) Z'–$\omega^{-1/2}$ linear plots in the low-frequency region derived from the EIS spectra (Fig. 4b), (b) Lithium-ion diffusion coefficients (D_{Li^+}) for each sample

In contrast, the NCM@BT electrode exhibited a delayed onset of non-linear coulombic efficiency and capacity fading compared to bare NCM. This indicates that the BT coating effectively acts as an interfacial stabilizer under high-voltage conditions. Consequently, the NCM@BT electrode demonstrates excellent capacity retention during long-term cycling, which contributes to an enhanced electrode lifespan.

Fig. 6a and 6b show the diffusion characteristics in the low-frequency region based on the EIS results shown in Fig. 4b. Specifically, they present the Z' vs. $\omega^{-1/2}$ plot and calculated Li^+ diffusion coefficient, respectively. The Warburg factor (σ) is obtained using Equation (1), and by substituting σ into Equation (2), the Li^+ diffusion coefficient (D_{Li^+}) can be determined [33,34].

$$Z' = R_1 + R_{ct} + \sigma\omega^{-1/2} \quad (1)$$

$$D_{Li^+} = R^2T^2/(2A^2n^2F^4C^2\sigma^2) \quad (2)$$

Here, Z' represents the real part of the impedance, R_1 the ohmic resistance at the electrolyte/electrode interface, R_{ct} the charge transfer resistance, and ω the angular frequency. In addition, R, T, A, n, F, and C denote the gas constant, absolute temperature, electrode area, number of electrons involved in the reaction, Faraday constant, and the molar concentration of Li^+, respectively.

The Warburg factor (σ) and the corresponding D_{Li^+} were calculated to be 41.5 and 0.87 × 10-17 cm^2 s^{-1} for the bare NCM sample and 26.7 and 1.80 × 10-17 cm^2 s^{-1} for the NCM@BT sample, respectively. Notably, the D_{Li^+} value for the NCM@BT sample was approximately 107% higher than that of the bare NCM, quantitatively confirming the significantly enhanced Li^+ diffusion performance.

Based on the comprehensive experimental results, the BT coating played a multifaceted role beyond that of a simple physical barrier, contributing to both interfacial electric field regulation and optimization of Li^+ diffusion pathways. The high dielectric constant of BT effectively modulates local electric fields at the electrode–electrolyte interface, alleviating Li^+ con-

centration gradients and thereby enabling more uniform and efficient ion transport [13,35]. In addition, the uniformly dispersed nanoscale BT particles simultaneously block direct contact with the electrolyte and perform a dual function of suppressing interfacial side reactions and enhancing Li^+ mobility [36]. This comprehensive interfacial modulation effect contributes to the maintenance of excellent interfacial stability and electrochemical reactivity, even under high-rate cycling conditions, which agrees well with the observed improvements in rate performance, reduced R_{ct}, and long-term cycling stability. Therefore, BT has been experimentally validated as a functional coating material that simultaneously enhances the interfacial stability and ion transport efficiency. These enhancements were achieved using the RAM process, which offers a simple and energy-efficient fabrication route and underscores the practical significance of this approach from a manufacturing perspective.

4. CONCLUSIONS

In this study, a functional dielectric coating strategy was proposed to simultaneously achieve interfacial stability and fast Li^+ transport under a high cut-off voltage of 4.5 V. The experimental results demonstrated that coating nanodot-structured ferroelectric $BaTiO_3$ (BT) on the surface of NCM811 significantly improved both high-rate performance and long-term cycling stability.

RAM, a solvent- and heat-free process, provides clear advantages in terms of simplicity, minimal particle damage, and scalability. Among the various BT coating contents, the 2 wt% sample exhibited the most favorable performance, delivering a 14.2% increase in capacity at 10 C, 51.8% reduction in charge transfer resistance (R_{ct}), and 107% enhancement in the Li^+ diffusion coefficient (D_{Li^+}). Additionally, it maintained 44.9% higher capacity retention after 200 cycles, indicating outstanding long-term cycling stability.

These performance enhancements are attributed to the dual role of BT as both a physical barrier that suppresses direct contact with the electrolyte and a dielectric layer that regulates the interfacial electric field distribution and mitigates local Li^+ concentration gradients, thereby simultaneously improving the interfacial stability and facilitating Li^+ diffusion.

This study presents a coating strategy that integrates high-permittivity dielectric materials with a facile, solvent-free RAM process, providing a practical interfacial design to mitigate high-voltage instability and promote the commercialization of next-generation high-energy lithium-ion batteries.

ACKNOWLEDGEMENT

This work was supported by the Technology Innovation Program (RS-2023–00256202, Development of MLCB design and manufacturing process technology for board mounting) funded By the Ministry of Trade, Industry & Energy (MOTIE, Korea).

REFERENCES

1. Meintz, A., *et al.*, "Enabling Fast Charging – Vehicle Considerations," *Journal of Power Sources*, 2017, 367, pp. 216–227.
2. Zhu, G.L., *et al.*, "Fast Charging Lithium Batteries: Recent Progress and Future Prospects," *Small*, 2019, 15(15), pp. e1805389.
3. Huang, Z., *et al.*, "Insights into the Defect-driven Heterogeneous Structural Evolution of Ni-rich Layered Cathodes in Lithium-ion Batteries," *Energy & Environmental Science*, 2024, 17(16), pp. 5876–5891.
4. Liu, W., *et al.*, "Nickel-rich Layered Lithium Transition-metal Oxide for High-energy Lithium-ion Batteries," *Angew Chem Int Ed Engl*, 2015, 54(15), pp. 4440–4457.
5. Ko, D.-S., *et al.*, "Microstructural Visualization of Compositional Changes Induced by Transition Metal Dissolution in Ni-rich Layered Cathode Materials by High-resolution Particle Analysis," *Nano Energy*, 2019, 56, pp. 434–442.
6. Xu, S., *et al.*, "Lithium Transport Through Lithium-ion Battery Cathode Coatings," *Journal of Materials Chemistry A*, 2015, 3(33), pp. 17248–17272.
7. Li, Y., *et al.*, "Toward a High-voltage Fast-charging Pouch Cell with TiO_2 Cathode Coating and Enhanced Battery Safety," *Nano Energy*, 2020, 71, pp. 104643.
8. Gao, H., *et al.*, "Modifying the Surface of a High-Voltage Lithium-Ion Cathode," *ACS Applied Energy Materials*, 2018, 1(5), pp. 2254–2260.
9. Negi, R.S., *et al.*, "Insights into the Positive Effect of Post-Annealing on the Electrochemical Performance of Al_2O_3-Coated Ni-Rich NCM Cathodes for Lithium-Ion Batteries," *ACS Applied Energy Materials*, 2021, 4(4), pp. 3369–3380.
10. Hu, Y., *et al.*, "Electrical Characterization of Amorphous $LiAlO_2$ Thin Films Deposited by Atomic Layer Deposition," *RSC Advances*, 2016, 6(65), pp. 60479–60486.
11. Wang, W., *et al.*, "Rational Design of a Piezoelectric $BaTiO_3$ Nanodot Surface-Modified $LiNi_{0.6}Co_{0.2}Mn_{0.2}O_2$ Cathode Material for High-Rate Lithium-Ion Batteries," *ChemElectroChem*, 2020, 7(17), pp. 3646–3652.
12. Liu, J., *et al.*, "Low-temperature Piezoelectric/ferroelectric Coating Layer Driving Lithium-ion Rapid Diffusion and Structure Stability of $LiCoO_2$ Cathode," *Journal of Electroanalytical Chemistry*, 2025, 979, pp. 118929.
13. Yasuhara, S., *et al.*, "Enhancement of Ultrahigh Rate Chargeability by Interfacial Nanodot $BaTiO_3$ Treatment on $LiCoO_2$ Cathode Thin Film Batteries," *Nano Lett*, 2019, 19(3), pp. 1688–1694.
14. Seo, J., *et al.*, "Enhancing Charge–Discharge Speed of Li-Ion Batteries with $BaTiO_3$-Coated $LiCoO_2$," *Journal of the Electrochemical Society*, 2024, 171(11).
15. Teranishi, T., *et al.*, "In situ Impedance Analysis on $BaTiO_3$–$LiCoO_2$ Composite Cathodes for Lithium Ion Batteries," *Japanese Journal of Applied Physics*, 2015, 54(10S).

16. Pélissier, K. and D. Thierry, "Powder and High-Solid Coatings as Anticorrosive Solutions for Marine and Offshore Applications? A Review," *Coatings*, 2020, 10(10).
17. Capece, M. and R.N. Davé, "Solventless Polymer Coating of Microparticles," *Powder Technology*, 2014, 261, pp. 118–132.
18. Bose, S. and R.H. Bogner, "Solventless Pharmaceutical Coating Processes: A Review," *Pharm Dev Technol*, 2007, 12(2), pp. 115–131.
19. Eyckens, D.J., *et al.*, "Solvent-free Surface Modification of Milled Carbon Fiber Using Resonant Acoustic Mixing," *Applied Surface Science*, 2024, 646.
20. Li, J., R. Yao, and C. Cao, "$LiNi_{1/3}Co_{1/3}Mn_{1/3}O_2$ Nanoplates with 010 Active Planes Exposing Prepared in Polyol Medium as a High-performance Cathode for Li-ion Battery," *ACS Applied Materials & Interfaces*, 2014, 6(7), pp. 5075–5082.
21. Li, D., *et al.*, "Microstructures and Electrochemical Performances of TiO_2-coated Mg–Zr co-doped NCM as a Cathode Material for Lithium-ion Batteries with High Power and long Circular Life," *New Journal of Chemistry*, 2021, 45(41), pp. 19446–19455.
22. Sim, S.J., *et al.*, "Use of Carbon Coating on $LiNi_{0.8}Co_{0.1}Mn_{0.1}O_2$ Cathode Material for Enhanced Performances of Lithium-ion Batteries," *Scientific Reports*, 2020, 10(1), pp. 11114.
23. Chen, J., *et al.*, "Enhanced Energy Storage Density in Poly(vinylidene fluoride-hexafluoropropylene) Nanocomposites by Filling with Core-shell Structured $BaTiO_3$@MgO Nanoparticals," *Journal of Energy Storage*, 2022, 53, pp. 105163.
24. Guan, P., *et al.*, "Enhancing Cyclic and In-air Stability of Ni-Rich Cathodes Through Perovskite Oxide Surface Coating," *Journal of Colloid and Interface Science*, 2022, 628(Pt B), pp. 407–418.
25. Teranishi, T., *et al.*, "Ultrafast Charge Transfer at the Electrode-electrolyte Interface via an Artificial Dielectric Layer," *Journal of Power Sources*, 2021, 494.
26. Xiong, C., *et al.*, "Enhanced Electrochemical Performance of $LiNi_{0.8}Co_{0.1}Mn_{0.1}O_2$ Cathode Material for Lithium ion Batteries by WO_3 Surface Coating," *International Journal of Electrochemical Science*, 2020, 15(9), pp. 8990–9002.
27. Wang, L., *et al.*, "A Novel Bifunctional Self-Stabilized Strategy Enabling 4.6 V $LiCoO_2$ with Excellent Long-Term Cyclability and High-Rate Capability," *Advanced Science (Weinh),* 2019, 6(12), pp. 1900355.
28. Chen, Y., *et al.*, "Improving the Cycling Stability of NCM811 at High-Voltage 4.5V in Ester-Based Electrolytes with LiDFOB," *Small Methods*, 2025, 9(4), pp. e2401178.
29. Wu, Z., *et al.*, "Ni-rich Cathode Materials for Stable High-energy Lithium-ion Batteries," *Nano Energy*, 2024, 126, pp. 109620.
30. Su, L., Z. Cui, and A., "Manthiram, Impact of High-Nickel Cathodes and Test Conditions on the Coulombic Efficiency of Lithium Metal in Advanced Electrolytes," *ACS Materials Letters*, 2023, 6(1), pp. 109–114.
31. Li, W., *et al.*, "Long-Term Cyclability of NCM-811 at High Voltages in Lithium-Ion Batteries: an In-Depth Diagnostic Study," *Chemistry of Materials*, 2020, 32(18), pp. 7796–7804.
32. Kumar, Y., *et al.*, "Redox-active Conductive Metal–organic Framework with High Lithium Capacities at Low Temperatures," *Journal of Materials Chemistry A*, 2024, 12(33), pp. 21732–21743.
33. Song, H., *et al.*, "Mo-doped LiV_3O_8 Nanorod-assembled Nanosheets as a High Performance Cathode Material for Lithium Ion Batteries," *Journal of Materials Chemistry A,* 2015, 3(7), pp. 3547–3558.
34. Dai, Z., *et al.*, "Surface Coupling between Mechanical and Electric Fields Empowering Ni-Rich Cathodes with Superior Cyclabilities for Lithium-Ion Batteries," *Advanced Science (Weinh)*, 2022, 9(18), pp. e2200622.
35. Lee, B.S., *et al.*, "Silicon/Carbon Nanotube/$BaTiO_3$ Nanocomposite Anode: Evidence for Enhanced Lithium-Ion Mobility Induced by the Local Piezoelectric Potential," *ACS Nano*, 2016, 10(2), pp. 2617–27.